crystals

MDPI

Article

Spectroscopy and Trace-Element Characteristics of Emeralds from Kamakanga, Zambia

Yi Zhang and Xiaoyan Yu *

School of Gemology, China University of Geosciences Beijing, 29 Xueyuan Road, Beijing 100083, China; zhangyi0186@163.com
* Correspondence: yuxy@cugb.edu.cn

Abstract: Currently, Zambia is the second largest source of emeralds, after Colombia. In this study, emerald samples from the Zambian Kamakanga deposit were examined by UV-Vis-NIR, Miro-FTIR, Diamond View^{TM}, and LA-ICP-MS. Representative UV-Vis-NIR spectra showed a distinct Fe^{3+} absorption peak, and the Fe-related absorption band was much stronger than that of the Cr-related absorption band. The infrared spectra showed that the absorption of type II H_2O was much stronger than that of type I H_2O. The results of LA-ICP-MS indicated that darker green, green, lighter green, and bluish-green emeralds had a clear separation of Cr/V (Cr/V > 15 for darker green, 10 < Cr/V < 15 for green, and Cr/V < 10 for lighter green and bluish green). In color zoning emerald, the contents of Cr, Sc, V, and Fe gradually increased with the intensity of the green color, while the opposite occurred for Cs. Cr is the main chromogenic element in Kamakanga emeralds. Additionally, Zambian Kamakanga emeralds contain high contents of total alkali metals (avg. 17,592 ppmw), Cs (avg. 1331 ppmw), Fe (avg. 8556 ppmw), Li (avg. 485 ppmw), Li + Cs (avg. 1816 ppmw), and Ga/Fe < 0.0025. Therefore, combined Fe versus Ga, Li versus Cs binary diagrams and K, Rb, and the Li + Cs ternary plot can distinguish Zambian emeralds from other important emerald origins.

Keywords: Zambian emerald; spectroscopy; trace-element characteristic

Citation: Zhang, Y.; Yu, X. Spectroscopy and Trace-Element Characteristics of Emeralds from Kamakanga, Zambia. *Crystals* **2023**, *13*, 1605. https://doi.org/10.3390/cryst13111605

Academic Editor: Malgorzata Holynska

Received: 23 October 2023
Revised: 14 November 2023
Accepted: 15 November 2023
Published: 20 November 2023

1. Introduction

Emerald is known as the "King of Green Gemstones" and is loved for its vibrant and beautiful color, which represents hope and the arrival of spring. In recent years, the Zambian production of emeralds has gradually increased, and Zambia is now the second largest source of emeralds, after Colombia [1–4]. However, compared those from Colombia, Zambian emeralds have not been systematically studied. Emerald deposits are found all over the world, and the main emerald sources are Colombia, Zambia, Brazil, Zimbabwe, Madagascar, and Afghanistan. The prices of emeralds with the same quality may differ, depending on their origins. Therefore, the market demand for identifying the origin of emeralds has gradually grown [5–8]. Origin identification has become an important part of the emerald evaluation system, which includes spectroscopy and trace-element tests.

Kamakanga is an emerald deposit in the Zambian Kafubu emerald area. Although the Zambian Kafubu emerald area was discovered and mined as early as 1928, large-scale mining and systematic research did not begin until the 1970s [3,4,9,10]. The deposits in this area were tentatively identified as schist-hosted, and the Zambian Kafubu area emeralds were similar to other schist-hosted emeralds around the world [11]. Subsequently, a brief description of the geological setting of the Zambian Kafubu area was reported by Sliwa et al. [9]. They concluded that the emerald deposits of this area are located in the ultramafic metamorphic rocks of the Muwa Supergroup, underlying the gneisses and granites of the basal mafic rocks and overlying the younger metamorphosed sedimentary rocks of the Katanga Supergroup [9]. The first geochemical and mineralogical data from the Kafubu emerald area were reported by Seifert et al. [2]. They concluded that mineralization of the Kamakanga emerald deposit occurred at 447 ± 8.6 Ma [2].

Emerald mineralization in the Kamakanga deposit is directly related to the metasomatic alteration of Cr-bearing metabasites by Be-bearing fluids in hydrothermal veins [3]. The rock in the Kamakanga deposit experienced magmatic intrusion during the Pan-African orogeny and, subsequently, the Be-rich magma and its derived fluids interacted with the nearby Cr- and V-rich host rock. Ultimately, emeralds formed within phlogopite reaction zones between the quartz–tourmaline veins and the metabasites [12]. Only 2% of the Zambian Kafubu emerald area is currently mined, and the Kamakanga emerald deposit is mined at the deepest depth (50–60 m). However, the results of a geological survey indicated that there are traces of emerald mineralization at a deeper level [2,4]. Consequently, the Kamakanga deposit still has the potential for the discovery of large and high-quality emeralds.

In recent years, experts have collected emeralds from the Zambian Kafubu area for spectroscopy study and analysis of chemical composition [3,13], and they have compared emeralds from this area with emeralds of other origins [14–19]. Actually, there are four mechanized mining deposits in the Zambian Kafubu emerald area—Kagem, Grizzly, Chantete, and Kamakanga. However, most of the research has been concentrated on the former three deposits, while few studies have been carried out on the Kamakanga deposit.

In this paper, we used an ultraviolet-visible near-infrared spectrophotometer (UV-Vis-NIR), Diamond View^{TM}, micro-fourier-transform infrared (Micro-FTIR) spectroscopy, and a laser ablation inductively coupled plasma mass spectrometer (LA-ICP-MS) to analyze emeralds from the Zambian Kamakanga deposit, so as to provide a more comprehensive scientific basis for identifying the origins of emeralds and to summarize and supplement the latest data.

2. Materials and Methods

2.1. Materials

Thirteen emerald samples (ZAKA-1 to ZAKA-13) were investigated from the Kamakanga deposit in Kafubu area, Zambia (Figure 1). Emerald samples were selected from more than 300 rough emeralds that were obtained from an owner of a local mine. Emerald samples were in the form of hexagonal columns, slabs, or fragments; they were slightly transparent to transparent, and green to bluish green in color.

Figure 1. The 13 different samples of emeralds studied.

2.2. Methods

The emerald samples were examined by UV-Vis-NIR spectra, color measuring, Miro-FTIR, Diamond View^{TM}, and LA-ICP-MS testing.

The UV-Vis-NIR spectra were recorded using a QSPEC GEM-3000 spectrophotometer manufactured by Biaoqi (Guangzhou, China) in the Gemological Research Laboratory of

the China University of Geosciences in Beijing (CUGB, Beijing, China) with the following specifications: between 360–1000 nm; spectral resolution, 0.5 nm; and integral time, 240–300 ms.

The color parameters were also collected by the QSPEC GEM-3000 spectrophotometer, with the following specifications: integral time, 242; scans to average, 10; boxcar width, 2; range of wavelength, 250–1000.

Micro-FTIR infrared spectroscopy was performed in reflection mode in the Gemological Research Laboratory of the China University of Geosciences in Beijing (CUGB, Beijing, China), between 4000–600 cm^{-1}. The micro-FTIR spectrometer model was a Bruker LUMOS (Ettlingen, Germany) with the following specifications: resolution, 4 cm^{-1}; scan time of background: 256; scan time of samples, 256; integration time, 80 s.

Diamond View™ (Maidenhead, United Kingdom), utilized at the Gemological Research Laboratory of the China University of Geosciences in Beijing (CUGB, Beijing, China), illuminated samples with hexagonal color zones.

The analysis of the in situ trace-element chemistry in the samples was completed at the National Research Center for Geoanalysis, Chinese Academy of Geological Sciences (CAGS), Beijing. The LA-ICP-MS analysis equipment consisted of an Applied Spectra IncJ-100 femto-second laser ablation system (343 nm) and a Thermo X-Series ICP-MS: laser spot diameters, 20 μm; laser frequency, 8 Hz; laser energy density, 1.08 J/cm^2; calibration reference materials, NISTSRM 610 and NIST SRM 612 (the mass discrimination and the time-dependent drift of sensitivity were corrected 1 time per 11 samples with calibration reference material). Internal standard element: ^{29}Si. Each analysis consisted of ~15 s of background acquisition of a blank measurement of gas, followed by 30 s of data acquisition from the sample. Chemical element analysis and calibration were completed using ICPMS Data Cal 10.8 software.

3. Results

3.1. Spectroscopy

3.1.1. Color Parameters

In gemology, the CIE 1976 LAB uniform color space is often used to represent the color of gemstones, and the color parameters include L* (lightness), C* (chroma value), h (hue angle), a*, and b*. All samples were tested with the GEM-3000 spectrophotometer. According to the results, the color parameters of the experimental samples were as follows: L* ∈ (33.76, 57.45), a* ∈ (−29.17, −1.36), b* ∈ (−1.50, 12.81), C* ∈ (1.36, 31.86), and h ∈ (144.6°, 189.5°) (Figure 2). The colors of the samples were mainly green; some samples had a bluish tinge in the blue-green tone interval, with medium lightness and low chroma.

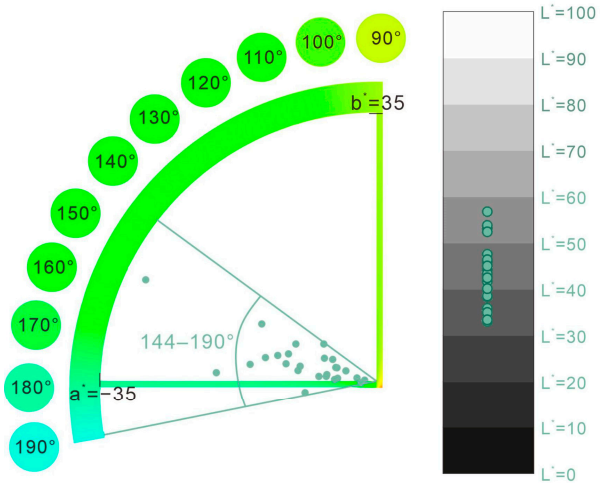

Figure 2. Color distribution of emerald samples in the CIELAB space. Modified from [20].

3.1.2. UV-Vis-NIR

Polarized spectra of the oriented samples were collected for obtaining the ordinary ray (o-ray) and the extraordinary ray (e-ray). All the emeralds showed similar bands for both the o-ray and e-ray. The representative UV-Vis-NIR spectra of Kamakanga emerald (ZAKA-7) are shown in Figure 3.

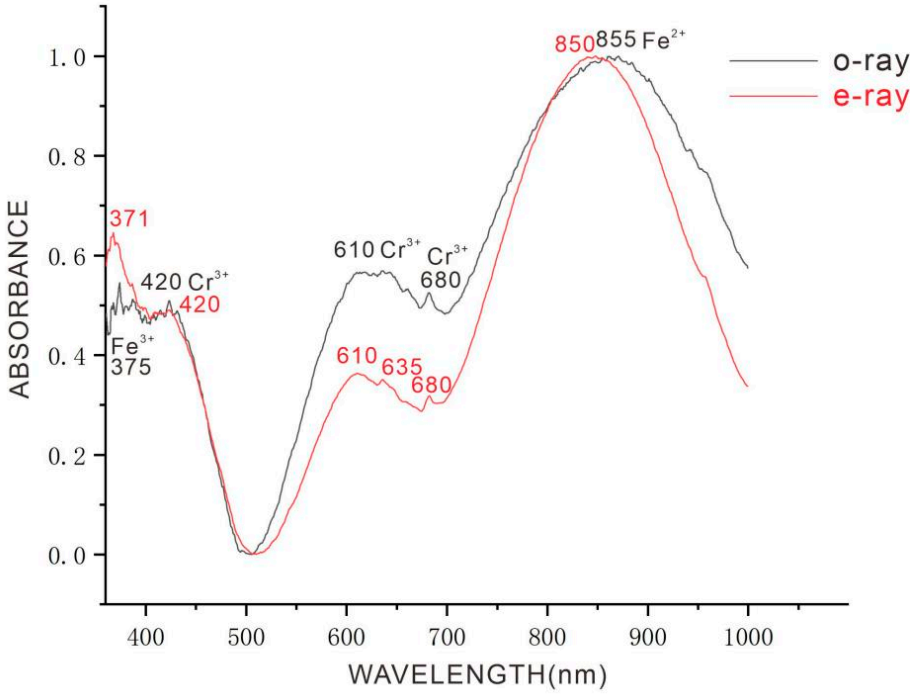

Figure 3. Representative UV-Vis-NIR spectra of Kamakanga emerald (ZAKA-7).

The o-ray (E⊥C) showed absorption bands at 420, 610–680, and 855 nm, as well as absorption peaks at 375 nm. The e-ray (E∥C) showed absorption bands at 420, 610–680, and 850 nm, as well as absorption peaks at 371 nm. The absorption bands and peaks at 420, 610, 635 and 680 nm indicated the presence of Cr^{3+}, which caused the green color [21]. In addition, Kamakanga emeralds are also abundant in Fe. The absorption peaks at 371 and 375 nm indicated the presence of Fe^{3+}, while the absorption bands at 850 and 855 nm indicated the presence of Fe^{2+} [22]. Kamakanga emeralds showed distinct absorption peaks at 371 and 375 nm, which were characteristic of high-Fe emeralds. The wavelength of the lowest absorption in the o-ray and e-ray spectra were essentially overlapping (~512 nm), indicating that the dichroism of Kamakanga emeralds was not strong.

3.1.3. Infrared Spectroscopy

According to the attribution of absorption peaks, the absorption peaks in the range of 3800 to 1400 cm^{-1} of the emerald infrared spectrum can be divided into three parts: the absorption peaks at 3800–3500 cm^{-1} are caused by channel water stretching vibration (Figure 4a); the absorption peaks at 3000–2000 cm^{-1} are caused by CO_2 or cedarwood oil (Figure 4b); the absorption peaks at 1700–1500 cm^{-1} are caused by channel water bending vibration (Figure 4c) [23,24].

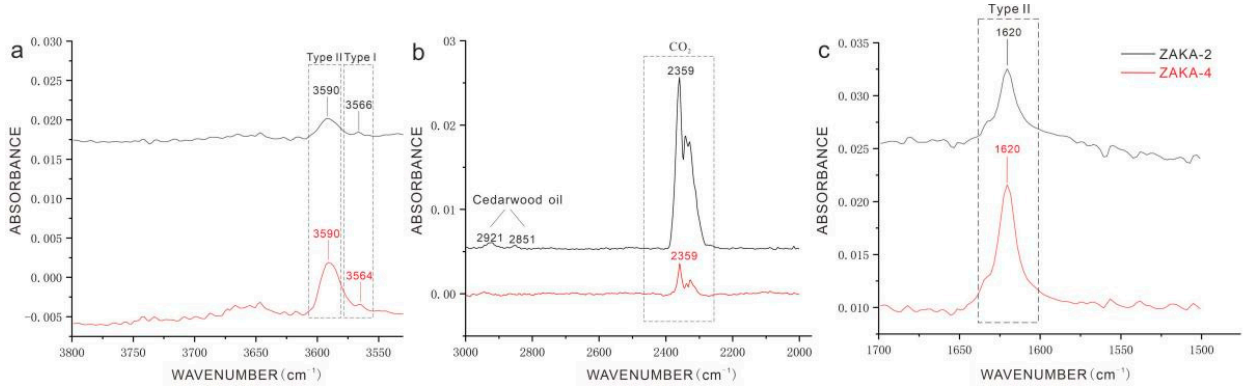

Figure 4. The representative infrared spectra (ZAKA-2 and ZAKA-4) in the range of (**a**) 3800–3500 cm^{-1}, (**b**) 3000–2000 cm^{-1}, and (**c**) 1700–1500 cm^{-1}.

As shown in Figure 4, the peaks at 3590 cm^{-1} of type I H_2O were sharp and strong, while the peaks at 3564 or 3566 cm^{-1} of type II H_2O were sharp but weak. The peak at 2359 cm^{-1} was caused by CO_2. The absorption peaks of cedarwood oil (2921 and 2851 cm^{-1}) were also shown in the infrared spectrum of ZAKA-2. The peak at 1620 cm^{-1} was caused by type I H_2O.

3.2. Trace-Element Analysis

Eleven regular emerald samples with different colors (ZAKA-1, 2, 4, 5, 6, 8, 9, 10, 11, 12, and 13) and one emerald sample with a multi-layered hexagonal color zoning (ZAKA-3) were selected and analyzed by LA-ICP-MS. The 11 regular samples were analyzed, and each sample was tested by two points. Color zoning sample appeared in varying shades of green in natural light, while under ultraviolet light excitation, the hexagonal growth color zoning also showed different shades of red fluorescence with clear boundaries (Figure 5). Consequently, seven separate tests (ZAKA-3-1 to ZAKA-3-7) (Table 1) were carried out at different color zones (nearly colorless, darker green, and lighter green).

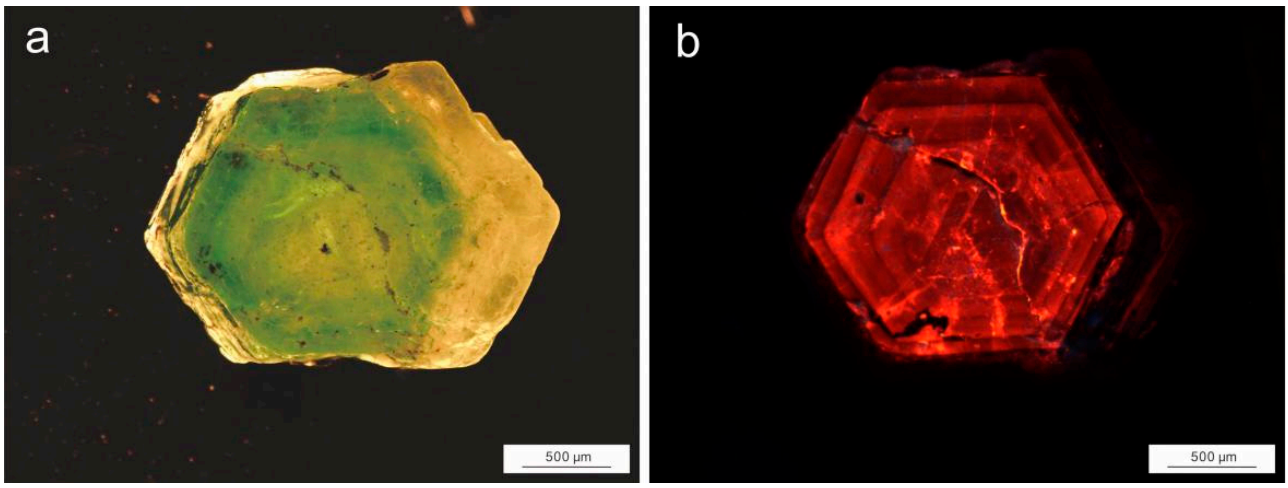

Figure 5. Color zoning sample (ZAKA-3) under (**a**) natural light and (**b**) ultraviolet light.

The results of LA-ICP-MS (Table 2) showed that Kamakanga emeralds from Zambia had stable and high contents of alkali metals (Li, Na, K, Rb, Cs) in the range of 15,120 to 20,407 ppmw (avg. 17,592 ppmw). The alkali metal concentrations, from highest to lowest, were Na, Cs, Li, K, and Rb. The Na contents ranged from 12,343 to 23,517 ppmw (avg. 15,981 ppmw); the Cs contents ranged from 626 to 2724 ppmw (avg. 1331 ppmw); the Li contents ranged from 301 to 843 ppmw (avg. 485 ppmw); the K contents ranged from 119 to 573 ppmw (avg. 369 ppmw); and the Rb contents ranged from 21 to 248 ppmw

(avg. 68 ppmw). Chromophore Cr, V, and Fe contents, respectively, ranged from 76 to 2934 ppmw (avg. 1435 ppmw), 78 to 183 ppmw (avg. 128 ppmw), and 5136 to 11,320 ppmw (avg. 8556 ppmw). The concentration of Cr was much higher than that of V and the Cr/V ratio was highly variable, ranging from 0.70 to 34.35. In addition, Zambian Kamakanga emeralds had high contents of Cs (avg. 1331 ppmw), Fe (avg. 8556 ppmw), and Li (avg. 485 ppmw).

Table 1. Chemical composition (average) of Kamakanga color zoning emerald by LA-ICP-MS (in ppmw).

Sample	ZAKA-3							Detection Limit
Element	1	2	3	4	5	6	7	
Li	244	514	322	291	300	262	229	7.0
Be	62,716	57,387	63,274	61,674	62,922	61,760	60,714	3.7
Na	16,527	15,707	17,449	16,143	15,115	15,480	16,731	7.5
Mg	13,958	14,580	14,673	12,847	12,008	12,596	14,857	3.5
Al	82,938	73,990	76,419	80,931	79,621	76,132	74,688	3.4
Si	286,062	299,557	288,163	289,069	290,512	293,697	295,428	58.0
P	44	30	54	44	20	31	46	3.7
K	82	398	710	236	278	321	408	5.8
Ca	bdl	285	440	369	259	361	265	30.9
Sc	227	48	35	136	146	181	9	0.2
Ti	77	84	74	71	77	79	73	0.6
V	156	105	57	123	122	143	77	0.1
Cr	1954	1212	767	1290	903	2001	85	2.2
Mn	5	12	23	6	5	7	6	0.4
Fe	6559	8572	9242	8542	7996	8220	6978	8.4
Co	5	2	7	6	6	6	5	0.1
Ni	12	11	31	15	20	25	15	2.6
Zn	21	16	24	25	21	23	17	2.4
Ga	19	13	12	16	16	17	14	0.2
Rb	33	74	30	24	22	25	33	0.4
Cs	404	626	427	457	441	342	623	0.1

bdl = below detection limit.

Table 2. Chemical composition (average) of Kamakanga regular emeralds by LA-ICP-MS (in ppmw).

Color	Bluish Green		Lighter Green		Green		Darker Green	
Sample	ZAKA-5 and 13		ZAKA-1, 4 and 6		ZAKA-2, 8 and 9		ZAKA-10, 11 and 12	
Element	Range	Avg.	Range	Avg.	Range	Avg.	Range	Avg.
Li	473–838	649	331–582	437	301–843	545	324–404	362
Be	47,416–58,296	52,258	52,317–56,811	55,199	52,338–57,387	55,026	49,916–56,252	53,966
Na	12,343–23,517	17,561	14,424–16,874	15,353	15,295–16,515	15,869	13,616–18,445	15,666
Mg	11,426–17,994	14,490	14,156–14,560	14,311	13,547–14,964	14,498	12,072–17,305	14,982
Al	69,846–95,352	82,489	71,083–77,271	72,736	69,264–77,901	73,403	70,369–81,793	74,764
Si	285,901–307,012	296,782	298,930–309,110	303,835	296,752–310,936	303,308	297,045–306,509	301,839
P	5–30	23	31–48	35	28–34	31	21–35	27
K	208–573	417	152–573	383	119–398	237	394–548	454
Ca	250–509	375	213–374	290	185–285	244	310–401	361
Sc	14–85	46	29–44	36	12–174	72	51–119	82
Ti	70–98	85	87–144	107	84–123	106	66–89	77
V	99–109	105	83–167	122	105–183	153	78–172	126
Cr	76–611	292	583–793	690	265–2463	1649	2582–2934	2727
Mn	15–29	23	7–15	12	12–16	14	19–29	23
Fe	8033–11,210	9719	6292–11,320	8748	5136–8848	7231	7879–9614	8912
Co	2–3	3	1–2	2	2	2	3–4	3
Ni	9–34	20	5–14	10	7–14	10	14–27	19
Zn	13–16	14	11–21	16	10–16	12	15–51	29
Ga	12–13	11	10–12	11	7–13	10	9–16	13
Rb	55–248	130	21–106	59	28–78	50	41–70	55
Cs	937–2025	1484	685–1664	1182	626–2724	1571	629–1956	1138

4. Discussion

4.1. Spectroscopy Characteristics

Emerald deposits can be roughly classified into two main groups (hydrothermal/metamorphic and schist-hosted/magmatic-related), according to their geological conditions of formation [12,25]. The UV-Vis-NIR spectra of the Kamakanga emerald have two characteristics: they contain a significant Fe^{3+} absorption peak (371 or 375 nm) and the Fe-related absorption band (850 or 855 nm) is much stronger than the Cr-related absorption band (420 nm and 610–680 nm). These two characteristics are typical of the UV-Vis-NIR spectra of schist-hosted emeralds, while the spectra of hydrothermal emeralds have no absorption peak at 371 or 375 nm and have no Fe-related absorption band at 850 or 855 nm (e.g., low-Fe Colombia emerald and low-Fe Afghanistan emerald) or Cr-related absorption band stronger than Fe-related absorption band at 850 or 855 nm (e.g., high-Fe China emerald, high-Fe Colombia emerald, high-Fe Afghanistan emerald) [26]. Therefore, UV-Vis-NIR spectra can be used to narrow down the range of emerald origins and to distinguish schist-hosted emeralds from hydrothermal emeralds. However, determining the geographic origin of schist-hosted emeralds requires the use of multiple lines of evidence, as well as the evidence provided bny UV-Vis-NIRspectra.

The peak positions and attributions of the Kamakanga emeralds in the infrared spectra are shown in Table 3. The absorption peaks of type II H_2O in Kamakanga emeralds are much stronger than those of type I H_2O, and some of the samples studied in this paper were filled with colorless oil. Infrared spectra showed that the channel water within the Kamakanga emeralds is mainly type II H_2O, which indicated that Kamakanga emeralds have a high content of alkali metal ions (15,120–20,407 ppmw; avg. 17,592 ppmw).

Table 3. Peak positions and attribution of the Kamakanga emeralds in infrared spectra (cm^{-1}).

Sample Number	Stretching Vibration				Cedarwood Oil	CO_2	Bending Vibration	
	Anti-Symmetric Stretching Vibration		Symmetric Stretching Vibration					
	I H_2O	II H_2O	I H_2O	II H_2O			I H_2O	II H_2O
ZAKA-2	-	-	3566	3590	2921, 2851	2359	-	1620
ZAKA-4	-	-	3564	3590	-	2359	-	1620
Previous study [23]	3700	-	-	3596	-	-	-	1622

4.2. Trace-Element Characteristics

The LA-ICP-MS results of 11 regular samples with different colors showed a wide variation of Cr/V (0.70 to 34.35) and a clear division of Cr/V for darker green, green, lighter green, and bluish green emeralds: Cr/V > 15 for darker green (15.84–34.35), 10 < Cr/V < 15 for green (10.77–14.86), and Cr/V < 10 (0.7–9.54) for lighter green and bluish green. However, the content of Cr (avg.1435 ppmw) was much higher than that of V (avg. 128 ppmw). This analysis indicated that Cr was the major chromogenic element in Kamakanga emeralds.

In addition, the variation of trace elements in different color zones of the color zoning sample (ZAKA-3) is shown in Figure 6. With the variation of colors (darker green color zoning → lighter green core → darker green color zoning → nearly colorless rim), the contents of Cr, V, and Sc showed large variability (Cr: 1954 → 767 → 2000 → 85 ppmw, Sc: 227 → 35 → 181 → 9 ppmw, V: 156 → 57 → 143 → 85 ppmw) (Figure 7). The trend was that the darker the green color, the higher the contents of Cr, Sc, and V, and the lower the content of Cs. However, the content of Cr was much higher than those of Sc, V, and Cs. In addition, Fe may have had a change in valence, so its content did not vary greatly with color. According to previous studies, the darker the green color, the higher the content of Fe [27]. Therefore, Cr is the main chromogenic element in Kamakanga emeralds, and Sc, V, Cs, and Fe may have some influence on the color of Kamakanga emeralds. Most trace-element contents were stable in the lighter green core and vary significantly in the darker green

color zoning and nearly colorless rim. This indicated that Kamakanga emeralds were grown in a stable environment during the early stages of mineralization.

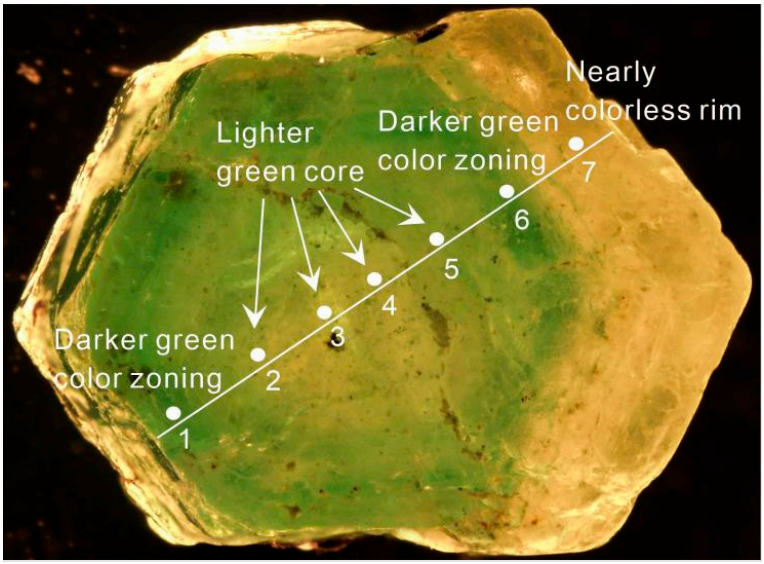

Figure 6. Representative photomicrograph of color zoning emerald ZAKA-3 with darker green color zoning, lighter green core, and nearly colorless rim. The white circles indicate the positions of analysis points corresponding to analyses of ZAKA-3-1 to ZAKA-3-7.

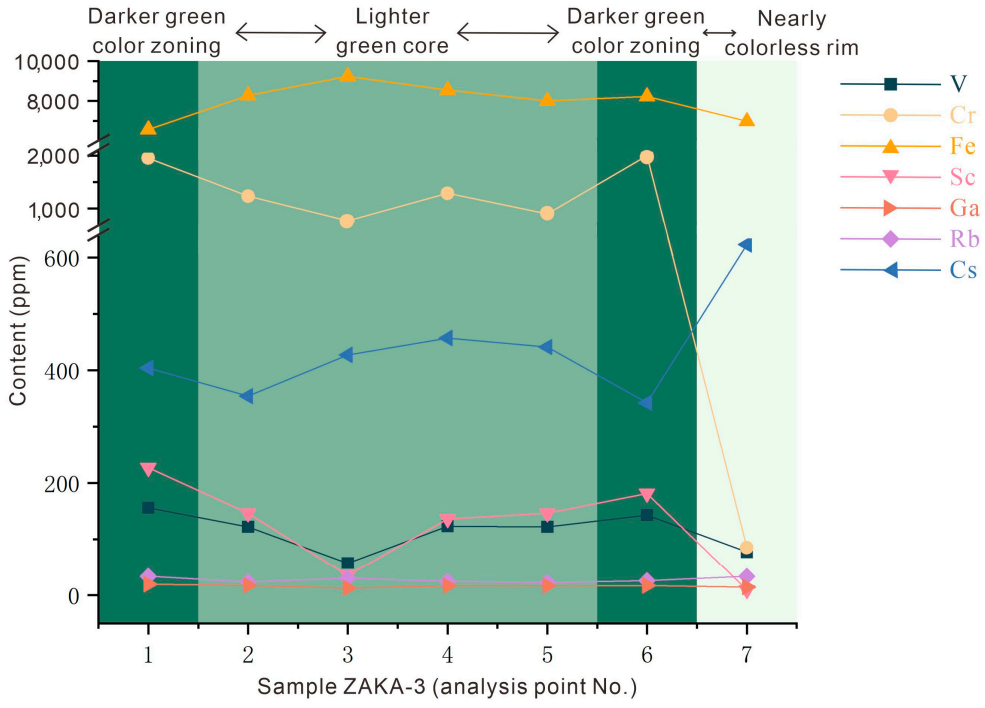

Figure 7. LA-ICP-MS data for selected trace-element analysis from ZAKA-3-1 to ZAKA-3-7. Plots of V, Cr, Fe, Sc, Ga, Rb, and Cs are used to highlight compositional changes, with uneven ordinate scales for clearer display.

Emerald deposits in different countries have different geological settings, so trace-chemical-element characteristics are essential for origin identification [15]. In order to distinguish the origin of emeralds further, by trace elements, the LA-ICP-MS data from this paper were analyzed and compared with data from other major emerald deposits in the world, and a series of binary diagrams and ternary plots of trace-element concentrations

were constructed (Figures 8–10). The data for the comparison came from the top six emerald origins, in terms of production (Colombia [28,29], Brazil [30], Zambia [28–30], Zimbabwe [29,30], Madagascar [29,31], and Afghanistan [28,29,32]), and from three origins with similar inclusion to that of Zambian Kamakanga emerald (India [18], Russia [29], Ethiopia [33]), and China [34], for a total of 139 sample data points.

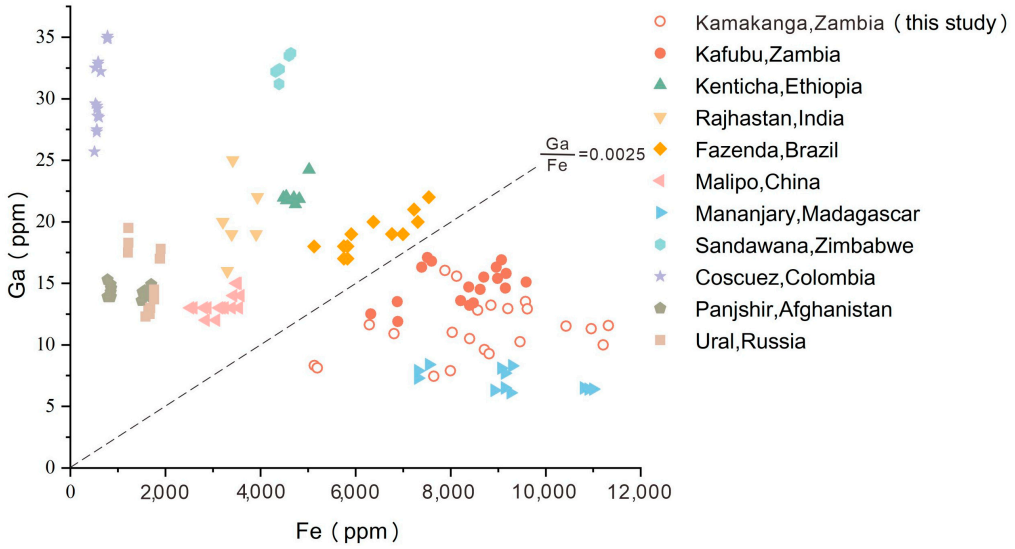

Figure 8. Plot of ferrum (Fe) versus gallium (Ga) concentrations from LA-ICP-MS analyses. Data are expressed in ppmw. Other sources are from [18,28–34].

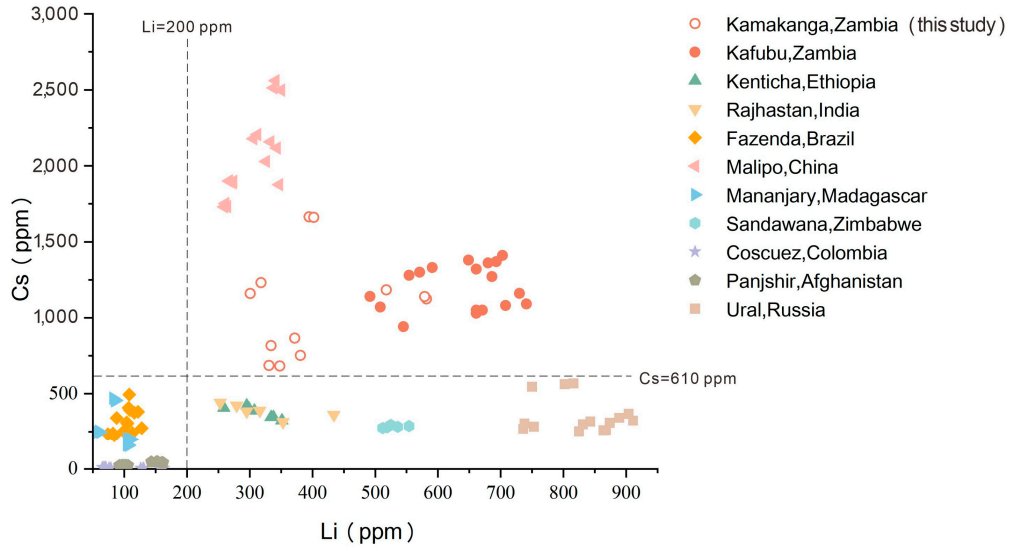

Figure 9. Plot of lithium (Li) versus cesium (Cs) concentrations from LA-ICP-MS analyses. Data are expressed in ppmw. Other sources are from [18,28–34].

As shown in the Fe versus Ga binary diagram (Figure 8), Zambian and Madagascan Ga/Fe < 0.0025, while the other origins are Ga/Fe > 0.0025. Zambian and Madagascan emeralds contain relatively high Fe (Zambian avg. 8556 ppmw; Madagascan avg. 9139 ppmw) and low Ga (Zambian avg. 11 ppmw; Madagascan avg. 7 ppmw). Consequently, Zambia emerald can be completely distinguished from other origins, except for Madagascar origins, by the Fe versus Ga binary diagram.

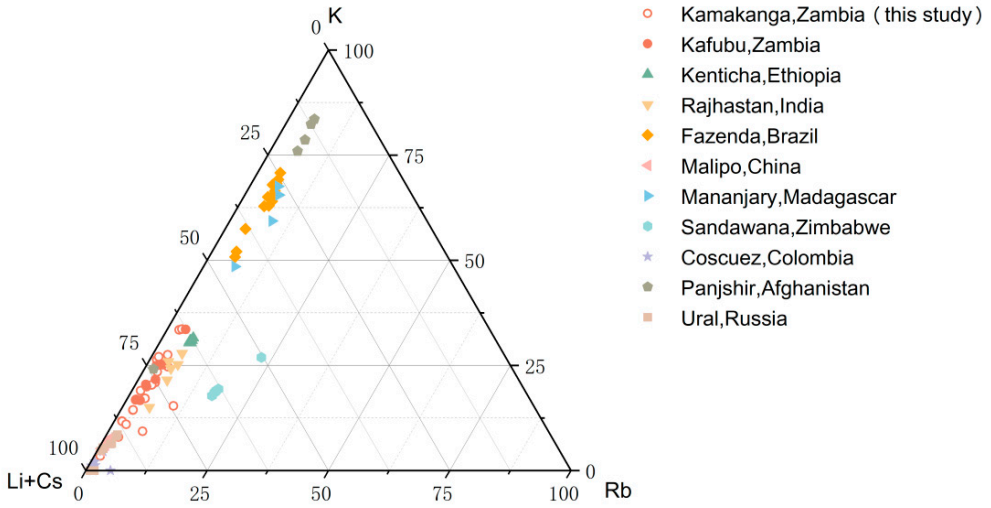

Figure 10. Ternary plot of relative abundance of klium (K), rubidium (Rb), and lithium + cesium (Li + Cs) in emerald samples from LA-ICP-MS analyses. Data are expressed in ppmw. Other sources are from [18,28–34].

Although Zambia and Madagascar partially overlap in the Fe versus Ga binary diagram, the two sources can be easily distinguished by the Li versus Cs binary diagram (Figure 9). This is because the contents of Cs (avg. 266 ppmw) and Li (avg. 89 ppmw) in Madagascar are much lower than the contents of Cs (avg. 1331 ppmw) and Li (avg. 485 ppmw) in Zambia.

Although India, Russia, Ethiopia, and Brazil emeralds have brownish platelet phlogopite and rectangular fluid inclusions that are similar to those of the Zambia emeralds [19], the Fe content in Russia emeralds (avg. 1618 ppmw) is much lower than that in Zambia emeralds (avg. 8556 ppmw). The contents of Cs (avg. 312 ppmw) and Li (avg. 103 ppmw) in Brazil are much lower than that in Zambia. The content of Cs in India (avg. 385 ppmw) is lower than that in Zambia. The content of Ga in Ethiopia (avg. 22 ppmw) is higher than that in Zambia (avg. 11 ppmw).

Zambia emerald can be easily distinguished from Madagascar, Brazil, and Afghanistan emerald by the ternary plot of relative abundance of K, Rb, and Li + Cs (Figure 10). Zambia emerald shows high content of Li + Cs (avg. 1816 ppmw), while Brazil and Madagascar emeralds show moderate contents of K and Li + Cs and Afghanistan emeralds show a high content of K. Bakakin and Belov [35] argued that when emeralds are enriched by Li, they also contain a higher concentration of Cs. In general, highly fractionated rare-element granitic pegmatites of the LCT association (Li, Cs, and Ta) are enriched in Li and Cs [30]. Zambia emeralds are, indeed, closely associated with highly fractionated pegmatites [2]. This indicates that the conclusions in this paper confirm those of previous studies.

5. Conclusions

This paper provides new data on the spectroscopy characteristics and the trace-element characteristics of Zambian Kamakanga emeralds. These data provide additional support for the identification of the origins of emeralds.

The UV-Vis-NIR spectra showed a distinct Fe^{3+} absorption peak, and the Fe-related absorption band was much stronger than the Cr-related absorption band. This confirmed that the Zambian Kamakanga emeralds are schist-hosted. The infrared spectra showed that the absorption peak of type II H_2O in Zambian emeralds is much stronger than that of type I H_2O, which indicated that the channel water in Zambian Kamakanga emeralds is mainly type II H_2O and the content of alkali metal ions in the emeralds is high.

LA-ICP-MS analysis showed that darker green, green, lighter green and bluish green emeralds have a clear separation of Cr/V (Cr/V > 15 for darker green, 10 < Cr/V < 15 for green, and Cr/V < 10 for lighter green and bluish green). In color zoning the emerald

the contents of Cr, Sc, V, and Fe were positively associated with the darkness of the green color, while Cs was negatively associated. Combining these two points, Cr is the main chromogenic element in Kamakanga emeralds, and Sc, V, Cs, and Fe have some influence on the color of Kamakanga emeralds. In addition, Zambian emeralds have a high content of total alkali metals (avg. 17,592 ppmw), Cs (avg. 1331 ppmw), Fe (avg. 8556 ppmw), Li (avg. 485 ppmw), Li + Cs (avg. 1816 ppmw), and Ga/Fe < 0.0025. Therefore, combined Fe versus Ga, Li versus Cs binary diagrams and K, Rb, and the Li + Cs ternary plot can distinguish Zambian emeralds from important emeralds of other origins.

Author Contributions: Conceptualization, Y.Z. and X.Y.; methodology, Y.Z. and X.Y.; software, Y.Z.; validation, Y.Z. and X.Y.; formal analysis, Y.Z. and X.Y.; investigation, Y.Z. and X.Y.; resources, X.Y.; data curation, Y.Z.; writing—original draft preparation, Y.Z.; writing—review and editing, Y.Z. and X.Y.; visualization, Y.Z. and X.Y.; funding acquisition, X.Y. All authors have read and agreed to the published version of the manuscript.

Funding: This study was financially supported by a project from the China Geological Survey (DD20190379-88).

Data Availability Statement: The data presented in this study are available in this article.

Acknowledgments: We are grateful to Mingke Wu for her support and technical guidance in the experiments. The authors are highly thankful to the reviewers and editors for their insightful and constructive comments, which helped to improve the manuscript.

Conflicts of Interest: The authors declare no conflict of interest.

References

1. Giuliani, G.; France-Lanord, C.; Coget, P.; Schwarz, D.; Cheilletz, A.; Branquet, Y.; Giard, D.; Martin-Izard, A.; Alexandrov, P.; Piat, D.H. Oxygen isotope systematics of emerald: Relevance for its origin and geological significance. *Miner. Deposita* **1998**, *33*, 513–519. [CrossRef]
2. Seifert, A.V.; Žáček, V.; Vrána, S.; Pecina, V.; Zachariáš, J.; Zwaan, J.C. Emerald mineralization in the Kafubu area, Zambia. *Bull. Geosci.* **2004**, *79*, 1–40.
3. Zwaan, J.H.; Seifert, A.V.; Vrána, S.; Laurs, B.M.; Anckar, B.; Simmons, W.B.S.; Falster, A.U.; Lustenhouwer, W.J.; Muhlmeister, S.; Koivula, J.I.; et al. Emeralds from the Kafubu Area, Zambia. *Gems Gemol.* **2005**, *41*, 117–148.
4. Mashikinyi, M. Investigating the Technical, Financial and Regulatory Challenges in the Zambian Gemstone Mining Sector: A Case Study of Gemcanton Investment Holdings Limited. Ph.D. Thesis, The University of Zambia, Lusaka, Zambia, 2020. Available online: http://dspace.unza.zm/handle/123456789/6853 (accessed on 22 October 2023).
5. Groat, L.A.; Giuliani, G.; Marshall, D.D.; Turner, D. Emerald deposits and occurrences: A review. *Ore Geol. Rev.* **2008**, *34*, 87–112. [CrossRef]
6. Marshall, D.; Pardieu, V.; Loughrey, L.; Jones, P.; Xue, G. Conditions for emerald formation at Davdar, China: Fluid inclusion, trace element and stable isotope studies. *Mineral. Mag.* **2012**, *76*, 213–226. [CrossRef]
7. Schwarz, D.; Klemm, L. Chemical signature of emerald. *Int. Geol. Congr. Abstr.* **2012**, *34*, 2812.
8. Vertriest, W.; Wongrawang, P. Gemological description of Ethiopian emeralds. *InColor* **2018**, *40*, 73–75.
9. Sliwa, A.S.; Nguluwe, C.A. Geological setting of Zambian emerald deposits. *Precambrian Res.* **1984**, *25*, 213–228. [CrossRef]
10. Zhang, B.L. *Systematic Gemmology*, 2nd ed.; Geology Press: Beijing, China, 2006; pp. 233–250.
11. Koivula, J.I. Tourmaline as an inclusion in Zambian emeralds. *Gems Gemol.* **1982**, *18*, 225–227. [CrossRef]
12. Giuliani, G.; Groat, L.A. Geology of corundum and emerald gem deposits: A Review. *Gems Gemol.* **2019**, *55*, 464–489. [CrossRef]
13. Ren, J.P.; Wang, J.; Zuo, L.B.; Liu, X.Y.; Dai, C.C.; Xu, K.K.; Li, G.Z.; Geng, J.Z.; Xiao, Z.B.; Sun, K.; et al. Zircon U–Pb and biotite40Ar/39Ar geochronology from the Anzan emerald deposit in Zambia. *Ore Geol. Rev.* **2017**, *91*, 612–619. [CrossRef]
14. Aurisicchio, C.; Conte, A.M.; Medeghini, L.; Ottolini, L.; De Vito, C. Major and trace element geochemistry of emerald from several deposits: Implications for genetic models and classification schemes. *Ore Geol. Rev.* **2018**, *94*, 351–366. [CrossRef]
15. Groat, L.A.; Giuliani, G.; Stone-Sundberg, J.; Sun, Z.Y.; Renfro, N.D.; Palke, A.C. A Review of Analytical Methods Used in Geographic Origin Determination of Gemstones. *Gems Gemol.* **2019**, *55*, 512–535. [CrossRef]
16. Long, Z.Y.; Yu, X.Y.; Zheng, Y.Y. Ore formation of the Dayakou emerald deposit (Southwest China) constrained by chemical and boron isotopic composition of tourmaline. *Ore Geol. Rev.* **2021**, *135*, 104208. [CrossRef]
17. Yu, X.Y.; Long, Z.Y.; Zhang, Y.; Qin, L.J.; Zhang, C.; Xie, Z.R.; Wu, Y.R.; Yan, Y.; Wu, M.K.; Wan, J.X. Overview of Gemstone Resources in China. *Crystals* **2021**, *11*, 1189. [CrossRef]
18. Qin, L.J.; Yu, X.Y.; Guo, H.S. Fluid Inclusion and Chemical Composition Characteristics of Emeralds from Rajasthan Area, India. *Minerals* **2022**, *12*, 641. [CrossRef]

19. Zhang, Y.; Yu, X.Y. Inclusions and Gemological Characteristics of Emeralds from Kamakanga, Zambia. *Minerals* **2023**, *13*, 341. [CrossRef]
20. Wang, H.; Guan, Q.; Liu, Y.; Guo, Y. Effects of transition metal ions on the colour of blue-green beryl. *Minerals* **2022**, *12*, 86. [CrossRef]
21. Wood, D.L.; Nassau, K. The characterization of beryl and emerald by visible and infrared absorption spectroscopy. *Am. Mineral.* **1968**, *53*, 777–800. Available online: http://pubs.geoscienceworld.org/msa/ammin/article-pdf/53/5-6/777/4255841/am-1968-777 (accessed on 22 October 2023).
22. Schmetzer, K.; Berdesinski, W.; Bank, H. Uber die Mineralart Beryll, ihre Farben and Absorptionsspektren. *Z. Dtsch. Gemmol. Ges.* **1974**, *23*, 5–39.
23. Taran, M.N.; Dyar, M.D.; Khomenko, V.M. Spectroscopic study of synthetic hydrothermal Fe^{3+}-bearing beryl. *Phys. Chem. Miner.* **2017**, *45*, 489–496. [CrossRef]
24. Zheng, Y.Y. Spectroscopy Charateristic of Channel Water and Origin Tracing of Dayakou Emerald from Yunan Province. Master's Thesis, China University of Geosciences, Beijing, China, 2020. (In Chinese).
25. Giuliani, G.; Groat, L.A.; Marshall, D.; Fallick, A.E.; Branquet, Y. Emerald deposits: A review and enhanced classification. *Minerals* **2019**, *9*, 105. [CrossRef]
26. Saeseaw, S.; Renfro, N.D.; Palke, A.C.; Sun, Z.; McClure, S.F. Geographic origin determination of emerald. *Gems Gemol.* **2019**, *55*, 614–646. [CrossRef]
27. You, Y.; Yu, X.Y.; Guo, H.S. Gemological Characteristics and Color Genesis of the Emeralds from Panjshir, Afghanistan. *China Gems Jades* **2021**, *167*, 2–8.
28. Saeseaw, S.; Pardieu, V.; Sangsawong, S. Three-phase inclusions in emerald and their impact on origin determination. *Gems Gemol.* **2014**, *50*, 114–133. [CrossRef]
29. Karampelas, S.; Al-Shaybani, B.; Mohamed, F.; Sangsawong, S.; Al-Alawi, A. Emeralds from the most important occurrences: Chemical and spectroscopic data. *Minerals* **2019**, *9*, 561. [CrossRef]
30. Zwaan, J.C.; Jacob, D.E.; Häger, T.; Neto, M.T.O.C.; Kanis, J. Emeralds from the Fazenda Bonfim region, Rio Grande do Norte, Brazil. *Gems Gemol.* **2012**, *48*, 2–17. [CrossRef]
31. Pardieu, V.; Sangsawong, S.; Cornuz, L.; Raynaud, V.; Luetrakulprawat, S. Update on Emeralds from the Mananjary-Irondro Area, Madagascar. *J. Gemmol.* **2020**, *37*, 416–425. [CrossRef]
32. Krzemnicki, M.S.; Wang, H.A.O.; Büche, S. A new type of emerald from Afghanistan's Panjshir Valley. *J. Gemmol.* **2021**, *37*, 474–495. [CrossRef]
33. Huang, Z.; Li, G.; Weng, L.Q.; Zhang, M.L. Gemological and Mineralogical Characteristics of Emerald from Ethiopia. *Crystals* **2023**, *13*, 233. [CrossRef]
34. County, M. Unique vanadium-rich emerald from Malipo, China. *Gems Gemol.* **2019**, *55*, 338–352.
35. Bakakin, V.V.; Belov, N.V. Crystal chemistry of beryl. *Geokhimiya* **1962**, *5*, 420–433.